Advanced Journal of Chemistry-Section A, 2020, 3(4), 422–431
Available online at : www.ajchem-a.com
ISSN Online: 2645-5676
DOI: 10.33945/SAMI/AJCA.2020.4.4

Original Research Article

Processing of Nanostructured TiO_2 and Modification of Its Photocatalytic Behavior for Methylene Blue Degradation

Mohammad Sajjadnejad[a,*], Hooman Karimi Abadeh[b]

[a] *Department of Materials Engineering, School of Engineering, Yasouj University, Yasouj, Iran*
[b] *Department of Materials Science and Engineering, School of Engineering, Shiraz University, Shiraz, Iran*

ARTICLE INFO

Received: 07 October 2019
Revised: 10 November 2019
Accepted: 15 November 2019
Available online: 08 December 2019

KEYWORDS

Sol-gel
TiO_2
Photocatalytic properties
Dip coating
Methylene Blue

ABSTRACT

In this work, sol-gel process was chosen to produce a photocatalytic film to degrade methylene blue. To study the structural and morphological properties, a base sol of TTIP, I-PrOH, and DEA were created. Then, with addition of 45 g/L PEG 2000, 30 g/L TiO_2, and 15 g/L PEG 2000+30 g/L TiO_2, three other additional sols were produced. The results of the thermogravimetry and differntial thermal analysis indicated that a calcination temperature of 550 °C is sufficient to calcinate all four layers formed in four sols. Structural X-ray studies showed that, calcination temperature is dependent of the composition. The results of this study revealed that, substrate will have an effect on the photocatalytic behavior. It was concluded that the rough sand blasted surface because of creating more film islands that enhances photocatalytic behavior is a better substrate surface condition. Degradation of Mb showed that as a result of more TiO_2 corporation in the film produced by the fourth sol, the fourth sol is superior in terms of photocatalytic behavior. Also it was found that, degradation of Mb is dependent on the initial concentration; and the higher initial concentration, the lower is the efficiency.

GRAPHICAL ABSTRACT

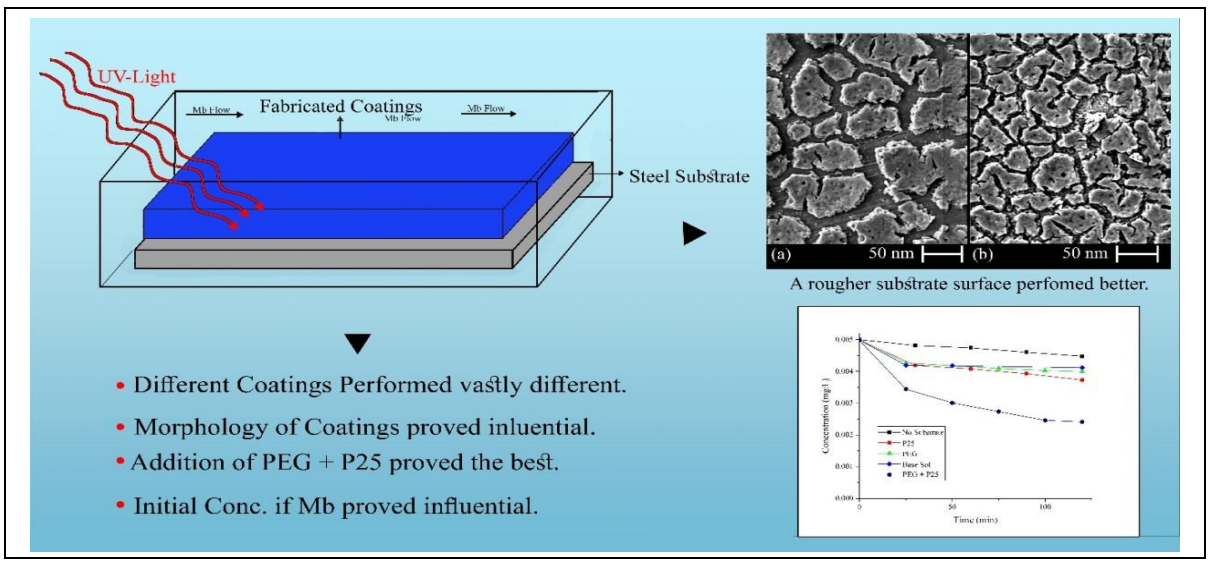

* Corresponding author's E-mail address: m.sajjadnejad@yu.ac.ir, m.sajjadnejad@yahoo.com

Introduction

TiO_2 has been used and studied extensively for its outstanding photocatalytic behavior [1-3]. Non-toxicity, chemical stability in aqueous environments, and inexpensiveness made this material a desirable semiconductor for industrial purposes. Due to inherent practical problems of using powder catalysts for water treatment and purification processes, i.e. homogenizing the powder throughout the whole medium and separation after treatment, immobilized TiO_2 films have been extensively researched and utilized.

Diverse techniques such as sputtering [4], electrospinning [2], chemical vapor deposition [5-7] and sol-gel [8-14] can be used to produce a desirable TiO_2 film. Among all these methods, sol-gel has been widely used due to its low cost, desirable homogeneity, and low processing temperature. There are two feasible methods for producing the TiO_2 films, the alkoxide route and non-alkoxide route. Inorganic salts ($TiCl_4$) are used in alkoxide route as the starting material for reactions, then after removing the inorganic anion of these salts results the desired TiO_2 from the film is achieved. However, halides are notoriously challenging to be removed and often remain in the material. The TiO_2 films produced by the non-alkoxide route possess high density and are crystalline [15].

Microstructure, density and phase identity of the film are the key factors in shaping the photocatalytic behavior of a film. The TiO_2 film produced from the mentioned process fabricated a network of material; so a calcination step should be carefully designed and undertaken to achieve the optimum photocatalytic properties, otherwise extensive deterioration of quality will occur.

Modified alkoxide sol-gel method has been extensively evaluated. The phenomena was first studied by Balasubramanian *et al.* [15] in 2004 and has stablished that a more sensitive TiO_2 photocatalyst can be produced by incorporating P-25 powder into an isopropoxide sol. Chen *et al.* [16,17] found out that this improvement is due to the grain reduction size, higher number of pores, micro-cracks and crystalline material on the surface of the coating. Polyethylene gelycol (PEG) addition to alkoxide solution and its beneficial application to increase the thickness of TiO_2 film and morpholgy was first reported by Kato *et al.* [18]. Many researches expanded this new finding and produced a rather well understanding of the PEG effect on TiO_2 film produced by sol gel method [19-22]. There are also many studies assessed the crystal size and phase transformation during the calcination steps [23,24].

One of the main organic pollutants of many industries such as pharmaceuticals, dyeing, printing, paper and ink industries is an organic solution called methylene blue (Mb). Fortunately, this aqueous contamination can easily be removed by using a photocatalysis method. There are several advantages in utilizing this route such as cost-effectiveness, solar light energy source, and operation near the ambient temperature.

The aim of this study is to synthesize nanostructured TiO_2 film using sol-gel containing both P-25 and PEG. Then the structure and morphology of the synthesized TiO_2 films to used as an effective photocatalyst to degrade Mb in environment were evaluated. It was found that, the TiO_2 powder (Degussa, P-25), is a standard material for photocatalytic applications, containing anatase and rutile phases in a ratio of about 3:1.

Experimental

Matrials and chemicals

TiO_2 films were produced using sol-gel method to study structural and morphological properties by XRD and SEM, respectively. To get clearer understanding of different affecting parameters, four different sols were prepared.

Table 1. Different materials used to create sols

Material	Original company and purity (%)	Chemical formula and molar mas
Titanium isopropoxide (TTIP)	Aldrich (97%)	$C_{12}H_{28}O_4Ti$ (284.215 g/mol)
Isopropyl alcohol (i-PrOH)	Merck (99.99%)	C_3H_8O (60.10 g/mol)
Diethylamine (DEA)	Aldrich (99%)	$C_4H_{11}N$ (73.14 g/mol)
Polyethylene glycol (PEG)	Merck (99.9%)	$C_{2n}H_{4n+2}O_{n+1}$(2000 g/mol)

Figure 1. Sols that were used in this study

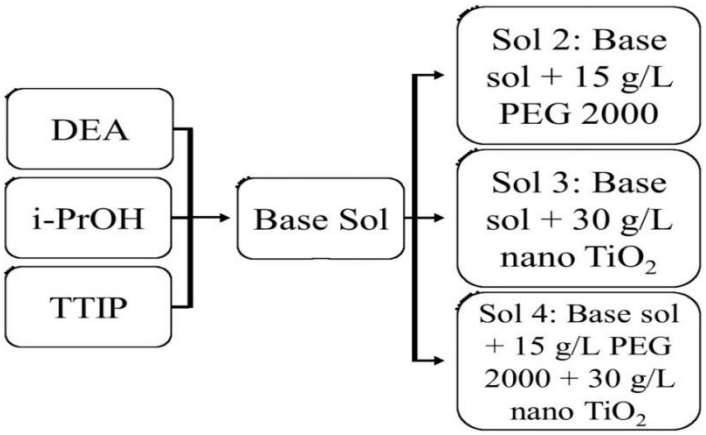

Table 1 presents the materials that were used to synthesize the sols. Methylene blue with the chemical formulae was used to assess which TiO_2 film possesses superior photocatalytic behavior.

Preparation of TiO_2 films by Sol-Gel method

A base sol and three derivative sols were prepared. To prepare the base sol, TTIP, i-PrOH and DEA were evaluated in terms of DEA:TTIP=4:1. Stirring was done for 2 h and then deionized water in terms of H_2O:TTIP=2:1 in molar ratio was added. To prepare the three other sols, 15 g/L PEG 2000, 30 g/L TiO_2 and 15 g/L PEG 2000+30 g/L TiO_2 were added to the base sol respectively. The ratios were chosen based on the reviewed literature [15-17]. Figure 1 schematically shows the constituents of different sols.

Dip coating method was utilized to produce the TiO_2 films required. Initially two substrates were used. 304 stainless steel and glass, 304 stainless steel showed preferential properties (for the reasons that will be explained) so the rest of the experiments were done on this substrate. The withdrawal rate was chosen to be 13.5 cm/min^{-1} and in order to increase film thickness 1 to 6 dipping cycles were performed. After each dip-coating cycle, specimens were dried for 2 h at 120 °C to obtain the crystallized anatase phase. Subsequently each sample was calcined in an oven at 400 °C to 700 °C. To minimize the nucleation of cracks in the coating surface, a slow heating rate of 3 °C/min^{-1} was chosen.

Characterization technique

To evaluate the thermal decomposition properties of the assynthesized dried zero gel samples, a thermogravimetry and differential thermal analyzer (PL-STA-1640, Polymer Labaratories Satntom Redcraft, UK) was used. By the means of a heating rate of 5 °C/min^{-1} temperature rose from 25 °C to 900 °C. X-ray diffraction (XRD) analysis was performed using an EQUINOX 3000 INEL with Cu (kα) radiation

to determine the present phases and crystalline size calculated from Debye-Scherrer equation [19].

$$L = \frac{k\lambda}{\beta \cos\theta}$$

Where L is crystalline size that is equal to multiplication of Debye-Scherrer constant (k=0.89) in the X-ray radiation wavelength (0.15481 nm for Cu (Kα)) divided by full-width half-maximum of diffraction (β) peak at 2θ. Morphology, thickness and chemical composition of the coatings were studied using scanning electron microscopy (SEX) (Seron Tech, AIS 2100) equipped with the energy dispersive X-ray spectroscopy (EDAX).

Results and discussion

TGA/DTA and UV-visible analysis

Figures 2 and 3 depict the overall weight loss curve if TGA/DTA for as-synthesized zero gel TiO_2. As can be seen in the TG curve (Figure 2), the total weight loss happens in several steps, the first of being at 12% between 25 to 235 °C as a result of removal of physisorbed water and solvent molecules from porous gel networks. The second step occurs at the temperature ranging from 235 to 450 °C and 30% weight loss was observed as a result of removal of DEA with boiling point of 268 °C [25]. In the third step, 15% weight loss was evident as a result of removal of strongly chemisorbed water molecules and residual organic species [1]. All these weight losses are proven by the small peaks that are showed in DTA curve (Figure 3). Amorphous to anatase TiO_2 transformation happens at 500 °C as a broad exothermic peak can be seen at this temperature. The curvature of the graph flattens beyond 550 °C which is an indication that a calcination temperature of 550 °C is enough to achieve the crystallization and removal of organic species.

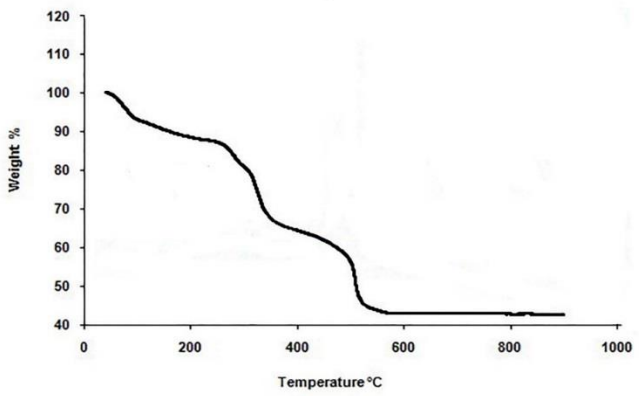

Figure 2. TG curve of the base sol derived TiO_2

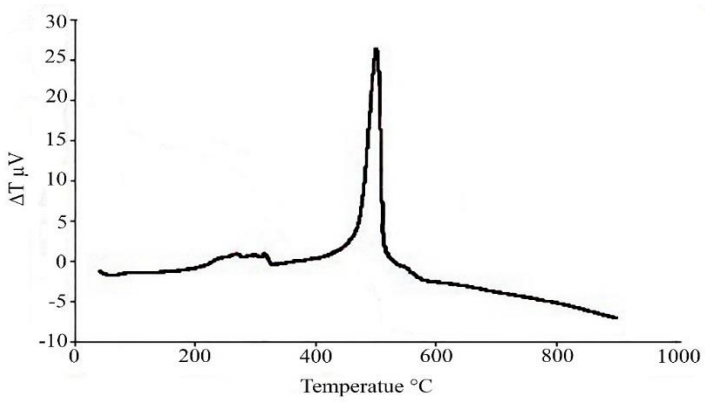

Figure 3. DTA curve of the base sol derived TiO_2

Structural Studies by X-ray

XRD patterns from the calcined base sol at different temperatures (400-700 °C) are shown in Figure 4. Two main peaks at 25.4° and 27.5° corresponded to the anatase (101) and rutile (110) peaks, respectively [13]. As the film was mostly amorphous before the calcination step, no distinctive peak can be seen before 400 °C; however, as calcination happens at 400 to 500 °C, sharper peaks can be seen as temperature rises. This is in agreement with the results of DTA analysis. The existence of other observable peaks such as anatase (200) and anatase (004) was an indication that the film was polycrystalline. According to these figures, anatase to rutile formation occurs at 500 to 600 °C, and at 700 °C the film is completely made of rutile.

To compare the phase transformation of base sol with other sols, forth sol (PEG+P25) was chosen for XRD analysis at the same temperatures of base sol. It was found that, the crystalline phases were observed even at 400 °C. This is the influence of P-25 addition that possesses anatase and rutile phases. The other interesting change that can be inferred is a distinctive shift in calcination temperature to 600-700 °C.

For the best photocatalytic behavior, the favorable anatase to rutile phase ratio is 70 to 30, thus there was a need in calculating the optimum calcination temperature. Crystallite sizes are presented in Table. It was found that, the crystallite size increased with temperature elevation. Crystallite sizes were calculated using the Scherrer's equation and anatase to rutile phase ratio was determined using the spur equation by utilizing peak intensities of anatase (101) and rutile (110).

$$F_A = 100 - \left\{ \frac{1}{1 + 0.8\left(\frac{I_A^{(101)}}{I_R^{(110)}}\right)} \right\} \times 100$$

Where F_A is the weight percentage of anatase phase and I_A and I_R are peak intensities of the anatase (101) and rutile (110), respectively. To achieve the optimum ratio desired, calcination temperature for the base sol determined to be between 500 to 600 °C and for the forth sol 500 °C. Agglomerated nanoparticles in the SEM micrographs of TiO_2 film immobilized in the base sol are presented in Figure 5.

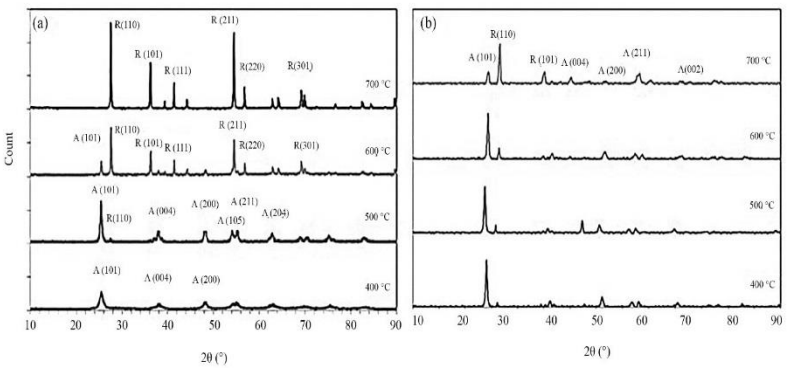

Figure 4. X-ray diffraction spectra of coatings from (a) the base and (b) fourth (containing PEG+P25) sols that were calcined at 400 °C to 700 °C

Table 2. Results from XRD measurements for TiO_2 films

Calcination temperature (°C)	Base sol crystallite size	Fourth sol crystallite size	Vol.% of anatase from base sol	Vol.% of anatase from fourth sol
400	30 (A)	19 (A)	100	74
500	35 (A)	21 (A)	92	71
600	42 (R)	21 (A)	18	67
700	52 (R)	24 (R)	-	28

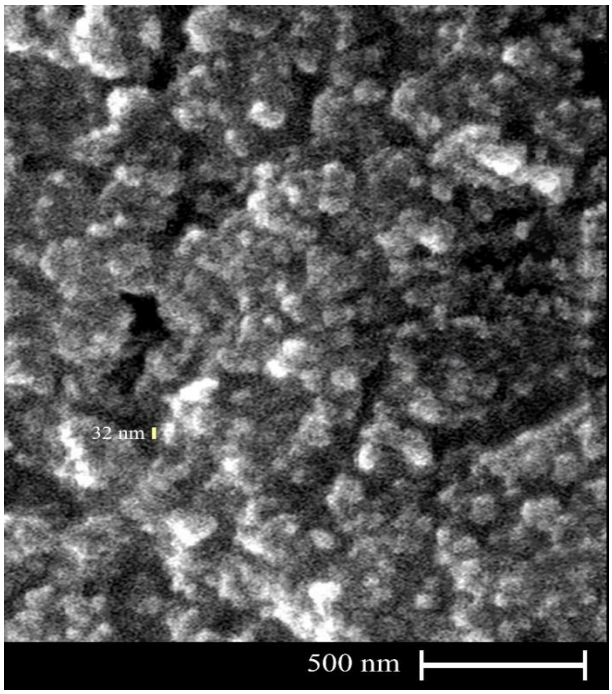

Figure 5. SEM image of the TiO_2 immobilized on stainless steel from the base sol (4 cycles)

Effects of substrate nature and condition on crack formation

To achieve a better understanding of the effect of surface roughness on the coated films, a smooth and rough sand blasted surface was utilized. Average diameter of the islands between cracks and the covered surface area were calculated using the Clemex software. Figure 6 a and b show that the rough sand blasted substrate possess smaller islands and smaller crack covered surface area as a result of more favorable condition for nucleation. This will lead to a more favorable condition for photocatalytic activity as it will increase the surface area available for the related reactions to happen, thus for the remainder of the study a rough sand blasted surface was chosen. The data extracted from Clemex software is presented in Table 3.

Effect of substrate on Mb degredation

Figure 7 depicts the morphology of the coatings that were produced by 4 cycles of dip-coatings from 4 different sols mentioned and then subsequently calcined at 500 °C. EDS studies (Figure 8) indicated that, the amount of TiO_2 in the film increased with addition of PEG and P-25. It theorized that this addition may increase the photocatalytic behavior of the films. To test this, degradation of Mb by photolysis was utilized. First, a small amount of Mb was degraded with no substrate and then the same test was performed with mentioned film substrate. As it can be inferred from Figure 9, photolysis of Mb was enhanced by addition of P-25. However, the best result was achieved in the in PED+P-25 film. In Figure 9, the vertical axis is the amount of maintained Mb in the solution, so as it decreased the degradation efficiency was improved.

Apart from the increased presence of TiO_2 in the film several other mechanisms are responsible for this behavior. P-25 loading produced more cracks on the film. This is the direct result of p-25's low permeability and high density that in turn decreases the permeability of TiO_2 film, thus formation of more cracks on the film [26]. On the other hand, PEG increases the roughness of the layer because of its removal during calcination step which lead to formation of more porosities [21]. Also, PEG limits water absorption in favor of direct dye absorption [27] not only at the surface of the photocatalytic film, but also at the increased porosities that are present in the film [28].

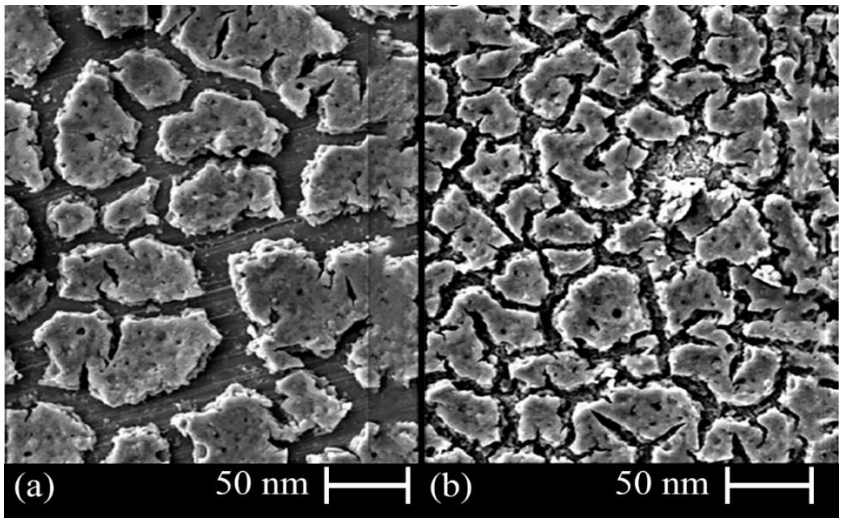

Figure 6. SEM images of the TiO_2 immobilized on (a) smooth and (b) rough stainless steel

Table 3. Average diameter of the islands and crack surface percentage that were calculated using Clemex software

	Sand blasted (rough)	Smooth
Crack area percentage	24%	35%
Average diameter of islands (μm)	60	37

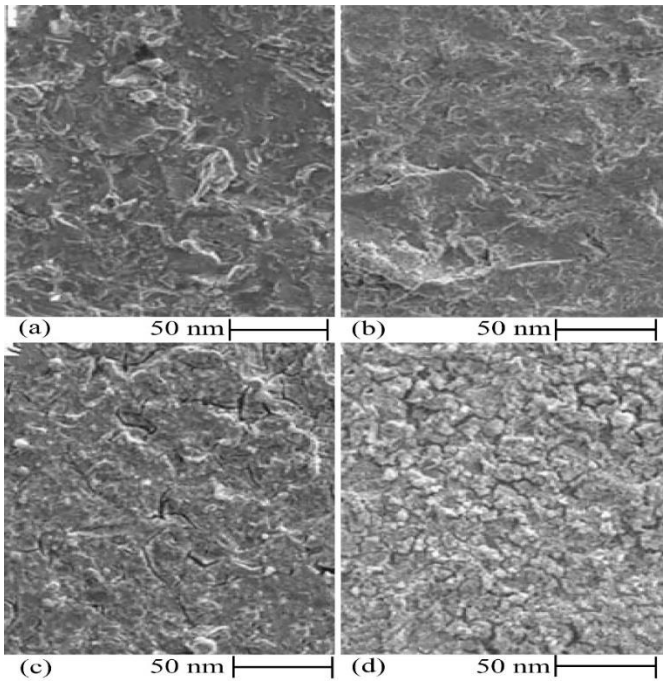

Figure 7. SEM images of the surface morphology of TiO_2 films immobilized from different sols

Effect of initial concentration of Mb

As seen in Figure 10, the photo degradation of Mb decreased as the initial concentration increased. Several other studies reported the same behavior for photo degradation of organic compounds and dyes [31, 32]. It was theorized that when the initial concentration of dye increased in the solution, the amount of absorbed Mb molecules on the surface of TiO_2 increased, limiting the direct interaction of other molecules with generated holes and

hydroxyl radicals. Also, a higher amount of Mb molecules in solution bulk absorbs an amount of UV light itself and lessen the amount of photons that reach the surface of TiO_2 film. This in turn decreased the hydroxyl radical flux [33] that ultimately resulted in a weaker degradation of Mb at higher initial concentrations.

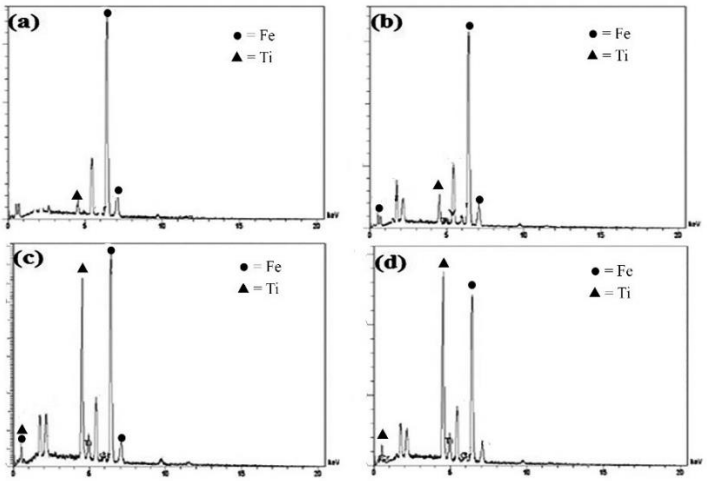

Figure 8. EDS analysis of the films produced from the (a) base sol (b) second sol (c) third sol and (d) fourth sol.

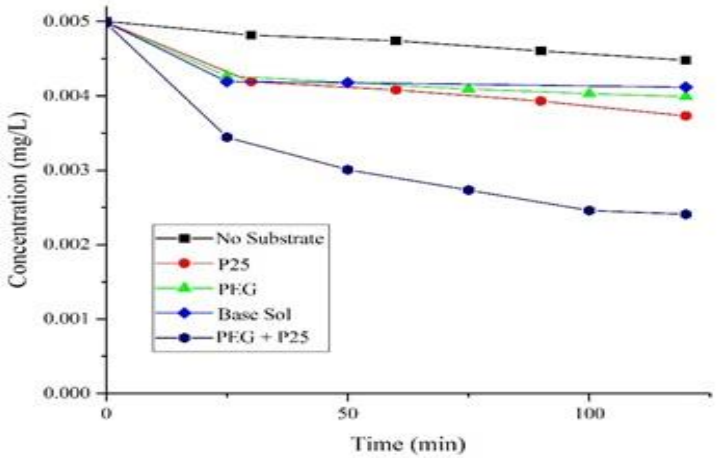

Figure 9. Photodegradation of Methylene blue on TiO_2 samples prepared from different sols

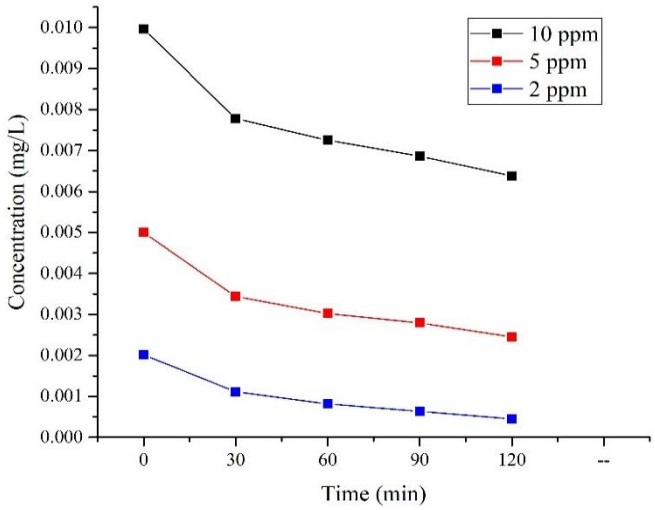

Figure 10. Effect of initial Mb concentration on photodegradation of Methylene blue

Conclusion

Sol-gel process was chosen to produce a photocatalytic film to degrade methylene blue. To study the structural and morphological properties fir souls were produced. Results of TGA/DTA tests indicated that a calcination temperature needed for four sols to calcinate. The XRD results revealed that, calcination temperature was dependent on composition. It was also found that, the substrate may affect the photocatalytic behavior and steel substrates with a sand blasted surface deemed superior. Additional tests indicated that, the increased dip coating cycles increased the nucleation and formation of cracks on the film. Degradation of Mb showed that as a result of more TiO_2 corporation in the film produced by the fourth sol, the photocatalytic behavior of the fourth sol is superior. The last tests of this research study indicated that, degradation of the Mb is dependent on the initial concentration and a higher initial concentration reduced the efficiency.

Disclosure statement

No potential conflict of interest was reported by the authors.

ORCID

M. Sajjadnejad **:** 0000-0001-5112-1791

References

[1] T. Sreethawong, S. Ngamsinlapasathian, S. Yoshikawa, *Chem. Eng. J.,* **2012**, *192*, 292–300.

[2] D. Li, C. Pan, *Progress Nat. Sci. Mater. Int.,* **2012**, *22*, 59–63.

[3] Y.P. Zhang, J.J. Xu, Z.H. Sun, C.Z. Li, C.X. Pan, *Progress Nat. Sci. Mater. Int.,* **2011**, *21*, 467–471.

[4] C.W. Lai, S. Sreekantan, P. San, E.W. Krengvirat, *Electrochim. Acta,* **2012**, *77*, 128–136.

[5] S. Mathur, P. Kuhn, *Surface Coat. Technol.,* **2006**, *201*, 807–814.

[6] V.G. Bessergenev, M.C. Mateus, D.A. Vasconcelos, J.F.M.L. Mariano, A.M. Botelho do Rego, R. Lange, E. Burkel, *Int. J. Photoenergy,* **2012**, 12.

[7] L. Ma, A. Chen, Z. Zhang, J. Lu, H. He, C. Li, *Catal. Commun.,* **2012**, *21*, 27–31.

[8] T.K. Tseng, Y.S. Lin, Y.J. Chen, H. Chu, *Int. J. Mol. Sci.,* **2010**, *11*, 2336–2361.

[9] D. Macwan, P.N. Dave, S. Chaturvedi, *J. Mater. Sci.,* **2011**, *46*, 3669–3686.

[10] P. Hartmann, D.K. Lee, B.M. Smarsly, J. Janek, *Acs Nano,* **2010**, *4*, 3147–3154.

[11] M.M. El-Nahass, M.H. Ali, A. El-Denglawey, *Trans. Non. Metal. Soc. China,* **2012**, *22*, 3003–3011.

[12] T. Zhang, T. Oyama, S. Horikoshi, J. Zhao, H. Hidaka, N. Serpone, *Solar Energy,* **2001**, *71*, 305–313.

[13] Y. Liang, H. Wang, H.S. Casalongue, Z. Chen, H. Dai, *Nano Res.,* **2010**, *3*, 701–705.

[14] M. Alzamani, A. Shokuhfar, E. Eghdam, S. Mastali, *Progress Nat. Sci. Materi. Int.,* **2013**, *23*, 77–84.

[15] G. Balasubramanian, D. Dionysiou, M. Suidan, V. Subramanian, I. Baudin, J.M. Laîné, *J. Mater. Sci.,* **2003**, *38*, 823–831.

[16] Y. Chen, D.D. Dionysiou, *Appl. Catal. A: General,* **2007**, *317*, 129–137.

[17] Y. Chen, D.D. Dionysiou, *Appl. Catal. B: Environ.,* **2008**, *80*, 147–155.

[18] K. Kato, A. Tsuzuki, Y. Torii, H. Taoda, T. Kato, Y. Butsugan, *J. Mater. Sci.,* **1995**, *30*, 837–841.

[19] Z. Su, L. Zhang, F. Jiang, M. Hong, *Progress Nat. Sci. Mater. Int.,* **2013**, *23*, 294–301.

[20] W. Huang, M. Lei, H. Huang, J. Chen, H. Chen, *Surface Coat. Technol.,* **2010**, *204*, 3954–3961.

[21] S.Q. Fan, C.J. Li, C.X. Li, G.J. Liu, G.J. Yang, L.Z. Zhang, *Mater. Trans.,* **2006**, *47*, 1703–1709.

[22] S. Bu, Z. Jin, X. Liu, L. Yang, Z. Cheng, *Mater. Chem. Phys.,* **2004**, *88*, 273–279.

[23] J. Yu, C.Y. Jimmy, W. Ho, Z. Jiang, *New J. Chem.,* **2002***, 26*, 607–613.
[24] J.G. Yu, H.G. Yu, B. Cheng, X.J. Zhao, J.C. Yu, W.K. Ho, *J. Phys. Chem. B,* **2003***, 107*, 13871–13879.
[25] E. Nouri, M. Shahmiri, H.R. Rezaie, F. Talayian, *Int. J. Indust. Chem.,* **2012,** *3*, 17.
[26] Y. Chen, D.D. Dionysiou, *Appl. Catal. B: Environ.,* **2006***, 62*, 255–264.
[27] L. Andronic, D. Perniu, A. Duta, *J. SolGel Sci. Technol*., **2013**, *66*, 472–480.
[28] Y. Kotani, T. Matoda, A. Matsuda, T. Kogure, M. Tatsumisago, T. Minami, *J. Mater. Chem.,* **2001***, 11*, 2045–2048.
[29] R.W. Matthews, *Water Res.,* **1990***, 24*, 653–660.
[30] H. Chun, W. Yizhong, T. Hongxiao, *Chemosphere,* **2000***, 41*, 1205–1209.
[31] I. Poulios, I. Aetopoulou, *Environ. Technol.,* **1999***, 20*, 479–487.
[32] C. So, M.Y. Cheng, J. Yu, P. Wong, *Chemosphere,* **2002***, 46*, 905–912.
[33] W.Z. Tang, H. An, *Chemosphere,* **1995***, 31*, 4157–4170.

How to cite this manuscript: Mohammad Sajjadnejad, Hooman Karimi Abadeh, Processing of Nanostructured TiO_2 and Modification of Its Photocatalytic Behavior for Methylene Blue Degradation*, Adv. J. Chem. A*, **2020**, *3*(4), 422–431.